UAV-Based Phenotyping of Nitrogen Responses in Winter Wheat: Grain Yield and Nitrogen Use Efficiency

Jingcheng Zhang[1,*], Kang Yu[1]

[1]Precision Agriculture Laboratory, School of Life Sciences, Technical University of Munich, Freising, Germany.

A paper from the Proceedings of the
16th International Conference on Precision Agriculture
21-24 July 2024
Manhattan, Kansas, United States

Abstract.

*Enhancing crop productivity through improved photosynthetic efficiency is crucial for global food security. This study investigates the relationships between six key photosynthetic parameters (i.e., intercellular CO_2 concentration (Ci), transpiration rate (E), quantum yield of photosystem II (PhiPS2), CO_2 assimilation (A), stomatal conductance (gs), and chlorophyll fluorescence (ChlF)), above ground biomass (AGB), chlorophyll content, canopy height, and grain yield (GY) at three critical growth stages of winter wheat. Advanced models, including Partial Least Squares Regression (PLSR) and Random Forest (RF), are used to predict GY and agronomic nitrogen use efficiency (aNUE) at three different growth stages. Early stage showed strong positive correlation between transpiration rate and stomatal conductance (r = 0.89***) and a negative correlation between photosynthesis rate and transpiration rate (r = -0.63***). In the medium stage, high correlations were observed among gs,E, and Ci (r = 0.97*** and r = 0.93***). Significant correlations between SPAD values and photosynthetic parameters are primarily observed in the late stage, indicating that higher chlorophyll content is associated with better photosynthetic efficiency and higher photosynthesis rates. A significant correlation between chlorophyll content and yield was observed in both the medium and late growth stages. A total of 35 different vegetation indices (VIs) related to chlorophyll, biomass, and photosynthesis were selected for analysis. Among these, NDVI, TVI, CTVI, RDVI, and RDVI_REG demonstrated strong positive correlations with both yield and chlorophyll content. Compared with PLSR, RF performed better in the aNUE estimation, highest accuracy was in the medium stage. Integrating photosynthetic parameters and vegetation indices enhances the prediction of grain yield and nitrogen use efficiency in winter wheat. The robust performance of PLSR and RF models supports their use in phenotypes monitoring, with key indicators such as AGB, PhiPS2, Ci, and Fv'/Fm' being vital for accurate aNUE and yield optimization. In summary, this research underscores the potential of different Nitrogen-related phenotypes in refining wheat cultivar yields and emphasizes the efficacy of UAV-enabled measurements for precise predictions associated with GY and NUE.*

Keywords.
Phenotyping, Unmanned Aerial Vehicle Systems (UAVs), Canopy Height, Grain Yield, Agronomic Nitrogen Use Efficiency (aNUE), Photosynthesis, Chlorophyll

Zhang, J. C. & Yu, K. (2024). UAV-Based Phenotyping of Nitrogen Responses in Winter Wheat: Grain Yield and Nitrogen Use Efficiency. In Proceedings of the 16th International Conference on Precision Agriculture (unpaginated, online). Monticello, IL: International Society of Precision Agriculture.

1.Introductions

Photosynthesis is the foundational process of energy capture and storage in organisms, driving vital cellular activities [1]. As the cornerstone of crop productivity, improvements in photosynthetic efficiency are directly linked to potential yield increases [2-5]. Enhancements in photosynthetic efficiency, particularly the rate of CO_2 assimilation (A) per leaf area can lead to yield increases [6]. It's encapsulating the efficiency of carbon assimilation by a plant through the photosynthesis, quantifying the balance of CO_2 uptake and O_2 release. The rate of CO_2 assimilation not only serves as a metric for photosynthetic activity but also acts as a comprehensive indicator of resource use efficiency [7,8], encompassing factors such as light [9], water [10], and nutrient availability [11]. Consequently, this measure serves as an essential indicator, crucial for assessing both crop productivity and the potential yield. Besides, stomatal conductance, denoted as 'gs', is also a vital physiological mechanism in plants that ensures gas exchange and significantly affects photosynthetic performance [12]. It facilitates the transfer of atmospheric CO_2 to mesophyll cells, where Rubisco catalyses CO_2 fixation in the Calvin-Benson-Bessam (CBB) cycle. Increasing the CO_2 concentration in the leaf can accelerate the CBB cycle and thus increase the rate of CO_2 assimilation [13]. Beyond CO_2 assimilation and stomatal conductance, chlorophyll fluorescence (ChlF) parameters, particularly PSII's maximum quantum efficiency in dark- and light-adapted states (Fv/Fm and Fv'/Fm'), serve as reliable indicators of photosynthetic efficiency [14], plant health [15], and stress detection [16]. Fv'/Fm' reflects the maximum energy conversion efficiency of PSII reaction centres when they are in the oxidized state [17]. A substantial number of publications cover the theoretical foundations of chlorophyll fluorescence analysis, emphasizing its value as a tool for studying the photosynthetic mechanisms [18,19]. In addition to these parameters, Intercellular CO_2 Concentration (Ci), which represents the concentration of CO_2 within the leaf's intercellular spaces, Transpiration Rate (E), which indicates the rate at which water vapor is lost from the plant to the atmosphere, and Quantum Yield of Photosystem II (PhiPS2), which measures the efficiency with which absorbed light is used for photochemistry in Photosystem II (PSII), are also important. These parameters collectively provide a comprehensive understanding of photosynthetic efficiency, plant health, and stress detection.

While these photosynthetic parameters provide insight into the immediate physiological responses of plants, it is AGB and canopy height offer cumulative measures of these processes over time. AGB represents the tangible outcome of photosynthetic activity—a synthesis of organic matter that is directly related to plant development and an essential determinant of yield [20,21]. Canopy height, on the other hand, serves as an indicator of plant vigor and growth dynamics, reflecting the overall health and productivity of the crop. Both AGB and canopy height serve as a comprehensive indicators for monitoring crop growth [22], predicting yield [23] and Agronomic Nitrogen Use Efficiency (aNUE) which is calculated by taking the difference between the crop yield with nitrogen fertilizer and the crop yield without nitrogen fertilizer, and then dividing this difference by the total amount of nitrogen applied[24]. The variations in AGB and canopy height among different wheat cultivars further illuminate the genetic and environmental interactions affecting crop productivity [25]. Therefore, a comparative analysis between AGB, canopy height and photosynthetic parameters is paramount to understand their respective roles and combined predictive power for winter wheat yield and aNUE, which is the focus of this study.

So far, precise, efficient, and objective plant phenotyping, including photosynthetic efficiency measurement, canopy height measurement, biomass estimation and yield prediction, has become a major focus of plant science [26,27]. However, traditional methods for assessing plant phenotyping are laborious and time consuming, which limits the sample analysis throughput [28]. Advances in the integration of Unmanned Aerial Vehicle Systems (UAVs) - derived datasets with advanced machine learning (ML) and deep learning (DL) algorithms [29] offers a promising frontier for enhancing the precision for GY [30], nitrogen uptake [31], senescence [32], plant density [33], and plant height [34].

Notwithstanding the application of UASs and associated vegetation indices (VIs) in the analysis of GY, little is known about what kind of the Nitrogen-related phenotyping traits is more important to predict grain yield. Moreover, the correlation between chlorophyll content, photosynthetic

activity and aNUE is not well-explored in the existing literature, adding another layer of complexity to understanding plant health and productivity.

This study postulated that higher chlorophyll content has a higher correlation with photosynthesis and can indicate a great capacity for yield production and nitrogen use efficiency. The objectives of this investigation are i) to examine the correlations between photosynthetic parameters, AGB, canopy height, chlorophyll content, and VIs with winter wheat grain yield and aNUE; ii) to evaluate the performance of selected VIs and ML models in predicting wheat yield and aNUE.

2.Materials and Methods

2.1 Study Area and Experimental Design

Seven diverse European winter wheat elite varieties were involved in this experiment, i.e., Aurelius (Saatbau Linz), Bernstein (Syngenta), Dagmar (Limagrain), Mv Nador (Marton genetics), Nogal (F. Desprez et Fils), Skyfall (R.A.G.T Saaten Deutschland), and Julius (KWS Lochow). These varieties were sown in plots that measured 10 m x 1.85 m, with a row spacing of 15 cm. The trial utilized a randomized complete block design, comprising four replicates and three nitrogen (N) treatments, resulting in a total of 84 plots. The experimental site was located at the research station of the Technical University of Munich in Dürnast, Freising (48.40630° N, 11.69535° E). The soil at this location is described as a homogeneous Cambisol with a composition of 20.8% clay, 61.5% silt, and 16.6% sand. Three N fertilizer levels (i.e., 0, 120, and 180 kg N ha^{-1}), which were chosen based on typical agronomic recommendations for winter wheat were implemented. These were applied in three equal portions around BBCH 25, 32, and 60 using Ammonium Sulphate Nitrate and Calcium Ammonium Nitrate. The soil was rich in P and K, so no additional application rate was added. Standard field management practices were uniformly applied across all plots. Sowing took place on 02.11.2022, and the crops were harvested upon reaching full maturity on 27.07.2023.

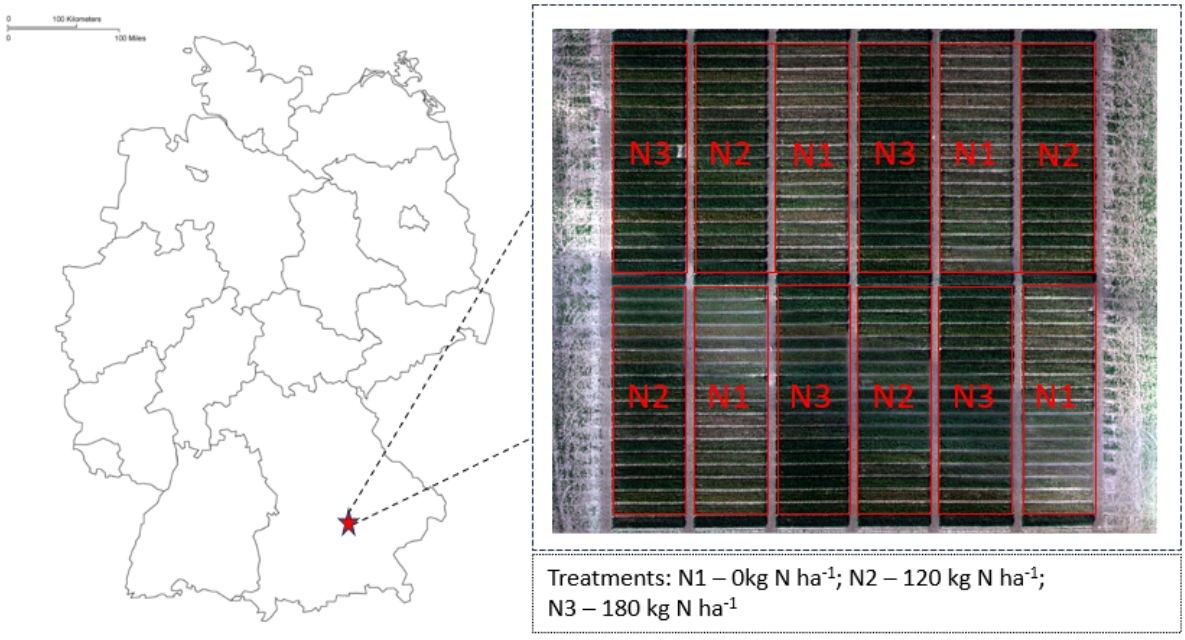

Fig 1 Location of the study area and overview of the experiment site. Different treatments are noted by N1 – 0 kg N ha^{-1}; N2 – 120 kg N ha^{-1}; N3 – 180 kg N ha^{-1}.

2.2 Data collection and acquisition

2.2.1. Photosynthetic Parameter Quantification

This investigation delineated the photosynthetic dynamics of selected European winter wheat

cultivars at critical phenological stages. Early (end of stem elongation), Medium (flowering), and Late (grain filling and maturation). The LI-6800 Portable Photosynthesis System (LI-COR Biosciences, Lincoln, NE, USA) facilitated the quantification of key photosynthetic metrics: net assimilation rate (A), stomatal conductance to water vapor (gsw), and the efficiency of photosystem II photochemistry as indicated by chlorophyll fluorescence (Fv'/Fm'). The LI-6800 provided data on four stomatal conductance parameters; however, this study focused on gsw due to its documented responsiveness to water related indices. Environmental conditions within the measurement chamber were rigorously regulated to ensure uniformity: airflow (700 µmol s^{-1}), relative humidity (55%), ambient CO_2 (400 ppm), chamber temperature (25°C), PAR (20 µmol $m^{-2}s^{-1}$), and light intensity for fluorescence measurements (1500 µmol $m^{-2}s^{-1}$). Measurements were taken post-equilibration, averaging 40 to 60 seconds per sample. Three foliar samples per plot were analyzed, with mean values used for subsequent analysis.

2.2.2. Chlorophyll Content Measurement

A SPAD-502 meter (Minolta Ltd, Osaka, Japan) was employed to obtain chlorophyll content. After calibrating the device, readings were taken from the first fully expanded leaf. Each leaf was measured three times, focusing on its upper, middle, and lower parts. In each plot, five random measurements were recorded, and their average determined the final value for that plot.

2.2.3. Acquisition and Processing of Multispectral Images

Reflectance data was captured using a DJI Matrice M300 RTK UAV, equipped with a MicaSense Dual Camera Kit. This setup captured data across ten spectral bands, namely: blue (444 nm, 475 nm), green (531 nm, 560 nm), red (650 nm, 668 nm), red edge (705 nm, 717 nm, 740 nm), and near-infrared (840 nm). Radiometric correction was ensured by an onboard ambient light sensor and reflectance panels used for calibration. UAV flights were conducted at 12 meters AGL for optimal GSD (1.08 cm) with 80% overlap in all directions. Flight timing was synchronized with peak solar irradiance for consistency. Orthomosaics were generated in Agisoft Metashape Professional 1.8.4, with geospatial accuracy verified by the UAV's RTK-GPS and SAPOS. Spectral band calculations on orthomosaics were performed in QGIS 3.32.3, employing raster calculator tools and Excess Green Index-based segmentation to minimize soil background interference. The refined spectral indices were saved as TIFF files for correlation analyses within the R environment. In this study, a comprehensive suite of 35 VIs was meticulously chosen to forecast the yield of winter wheat cultivars. These Vis are related to photosynthesis, AGB, and chlorophyll content. The aggregation of these indices was aimed at harnessing their collective predictive power to enhance the accuracy of yield estimations, thereby addressing the critical intersection of photosynthetic activity and biomass accumulation. Computations were conducted in Python, using the 'rasterio' package to manage zonal statistics and calculate mean VI values for defined AOIs corresponding to experimental plots.

2.2.4. Modelling Approaches and Evaluation

Partial Least Squares Regression (PLSR) and Random Forest (RF) were employed to discern predictive relationships between VIs and empirical phenotyping data. Correlation analyses and model constructions were performed using various Python packages, including ‘pandas’, ‘numpy’, ‘scikit-learn’, ‘matplotlib’, and ‘seaborn’. Data was partitioneed into training and test sets with extensive cross-validation to ensure model validity. Model accuracy was evaluated using coefficient of determination (R^2) (1), and Root Mean Square Error (RMSE) (2), with higher R^2 and lower RMSE indicating improved model precision.

$$R^2 = 1 - \sum_{i=1}^{n}(y_i - \hat{y}_i)^2 \;/\; \sum_{i-1}^{n}(y_i - \bar{y})^2 \quad (1)$$

$$RMSE = \sqrt{{}^{1}/_{k} \sum_{i=1}^{n}(x_i - y_i)^2} \quad (2)$$

3.Results and Discussions

3.1 Correlation analysis among photosynthesis parameters, Above Ground Biomass (AGB), SPAD, height, Agronomic Nitrogen Use Efficiency (aNUE) and Grain Yield (GY)

Table 1. Correlation analysis among photosynthesis parameters, Above Ground Biomass (AGB), SPAD, height, Agronomic Nitrogen Use Efficiency (aNUE) and Grain Yield (GY) in different stages.

Stages	Parameters	A	Ci	gsw	E	PhiPS2	Fv'/Fm'	SPAD	AGB	GY	aNUE	Height
Early	A	1.00***										
	Ci	0.03	1.00***									
	gsw	-0.27*	-0.07	1.00***								
	E	-0.63***	-0.13	0.89***	1.00***							
	PhiPS2	-0.53***	-0.10	0.42**	0.63***	1.00***						
	Fv'/Fm'	-0.50***	-0.14	0.38**	0.58***	0.93***	1.00***					
	SPAD	0.16	0.06	-0.21	-0.23	-0.09	-0.13	1.00***				
	Biomass	0.28*	-0.02	-0.08	-0.20	-0.30*	-0.29*	0.26*	1.00***			
	Yield	0.17	-0.15	-0.20	-0.21	-0.13	-0.02	0.28*	0.24	1.00***		
	aNUE	0.04	0.16	0.12	0.07	-0.03	-0.05	0.02	0.04	0.33*	1.00***	
	Height	0.12	-0.12	-0.18	-0.20	-0.16	-0.06	-0.18	0.31*	0.14	-0.06	1.00***
Medium	A	1.00***										
	Ci	0.41**	1.00***									
	gsw	0.51***	0.93***	1.00***								
	E	0.51***	0.94***	0.97***	1.00***							
	PhiPS2	0.30*	0.33*	0.40**	0.28*	1.00***						
	Fv'/Fm'	0.36**	0.29*	0.39**	0.27*	0.97***	1.00***					
	SPAD	-0.02	0.17	0.16	0.20	-0.14	-0.13	1.00***				
	Biomass	0.16	0.09	0.12	0.18	-0.08	-0.03	0.16	1.00***			
	Yield	0.04	-0.15	-0.09	-0.06	-0.21	-0.13	0.51***	0.24	1.00***		
	aNUE	0.08	-0.09	-0.00	0.01	0.05	0.09	-0.17	0.11	0.33*	1.00***	
	Height	0.10	-0.12	-0.06	-0.08	-0.11	-0.07	0.07	0.27*	0.16	-0.16	1.00***
Late	A	1.00***										
	Ci	0.24	1.00***									
	gsw	0.32*	0.19	1.00***								
	E	-0.07	-0.13	0.89***	1.00***							
	PhiPS2	0.17	-0.28*	0.05	0.09	1.00***						
	Fv'/Fm'	0.03	-0.47***	0.07	0.20	0.91***	1.00***					
	SPAD	0.46**	-	0.04	0.00	0.28*	0.40**	1.00**				

	*	0.49***					*				
Biomass	-0.11	-0.37**	-0.11	-0.01	0.17	0.30*	0.35**	1.00***			
Yield	0.40**	-0.23	-0.01	-0.09	0.36**	0.43***	0.74***	0.44***	1.00***		
aNUE	0.09	0.13	0.18	0.11	0.07	0.05	0.01	0.14	0.33*	1.00***	
Height	0.14	-0.46***	-0.35**	-0.31*	0.20	0.18	0.42**	0.13	0.15	-0.19	1.00***

Note: "***" indicates a significance level of $p < 0.001$ (highly significant); "**" indicates a significance level of $p < 0.01$ (very significant); "*" indicates a significance level of $p < 0.05$ (significant); "." indicates a significance level of $p < 0.1$ (marginally significant); no symbol indicates that the correlation is not statistically significant (n.s.).

The correlations were examined between photosynthetic parameters (A, gsw, Fv'/Fm', Ci, E, PhiPS2), AGB, chlorophyll content, canopy height, and GY at three critical growth stages (Table 1). During the early stage, a strong positive correlation exists between transpiration rate and stomatal conductance, indicating that higher transpiration rates are associated with higher stomatal conductance (r = 0.89***). Conversely, a significant negative correlation is observed between photosynthesis rate and transpiration rate (r = -0.63***), suggesting that increased photosynthesis may be linked to reduced transpiration. Additionally, PhiPS2 and Fv'/Fm' exhibit strong positive correlations with each other and with transpiration rate, emphasizing the interdependence of photosynthetic efficiency parameters. Yield shows a notable positive correlation with chlorophyll content (r = 0.28*), implying that higher chlorophyll content could contribute to increased grain yield.

In the medium stage, there are very high positive correlations among stomatal conductance, transpiration rate, and intercellular CO_2 concentration (Ci), indicating that these parameters are closely linked (gsw and E, r = 0.97***; gsw and Ci, r = 0.93***). The strong relationship between PhiPS2 and Fv'/Fm' persists (r = 0.97***). Notably, yield continues to demonstrate a significant positive correlation with chlorophyll content (r = 0.51***), reinforcing the importance of chlorophyll content in enhancing grain yield during this growth stage.

In the late stage, the photosynthesis rate shows a significant positive correlation with chlorophyll content (r = 0.46***), suggesting that increased photosynthetic activity is associated with higher chlorophyll levels. GY exhibits significant positive correlations with several parameters, including AGB, PhiPS2, Fv'/Fm', and chlorophyll content. These relationships indicate that higher biomass and efficient photosynthesis contribute to better grain yield outcomes. Interestingly, plant height shows strong negative correlations with intercellular CO_2 concentration and stomatal conductance highlighting potential trade-offs between plant height and these physiological parameters.

The relationship between Vegetation Indices and photosynthesis parameters, AGB, SPAD, height, aNUE and GY in different stages was examined through linear regression analysis in different growth stage. Across all growth stages, vegetation indices such as NDVI, TVI, CTVI, RDVI, and RDVI_REG consistently show strong positive correlations with yield and chlorophyll content, suggesting they are reliable indicators for predicting crop performance. These indices are also inversely related to water loss parameters (E and gsw), indicating their potential role in identifying crops with better water use efficiency. Conversely, indices like NDWI show strong negative correlations with yield and chlorophyll content, suggesting that while they might be useful for other applications, they are not favorable indicators for high yield or chlorophyll content in this context.

3.2 Yield and aNUE Prediction models

3.2.1. Partial Least Square Regression

The PLSR models for aNUE, depicted in Fig.2 (a) to (c), exhibit relatively low predictive power with one component, suggesting that a more complex model might be necessary to capture the variability in aNUE. The low R^2 and high RMSE values indicate that the single-component models

do not effectively predict aNUE.

In contrast, the PLSR models for Grain Yield, shown in Fig.2 (d) to (f), demonstrate substantial predictive accuracy. The models with 4 and 6 components show high R^2 values (ranging from 0.91 to 0.95) and relatively low RMSE (ranging from 697.67 to 823.63), indicating a strong alignment between predicted and actual yield values. The reference to the medium and late stages highlights the effectiveness of PLSR at different growth stages, particularly emphasizing the improved predictive accuracy as the crop approaches maturation.

The choice of the number of components in the PLSR models is guided by the "elbow point" method, which strategically reduces RMSE values by selecting the optimal number of components that capture the maximum variance with the least error. This method helps in balancing model complexity and predictive accuracy, ensuring the model is neither overfitted nor underfitted.

Overall, the analysis supports the use of PLSR for yield prediction, particularly in later growth stages, where the model's ability to integrate complex spectral data proves advantageous. The strong correlation coefficients with AGB further reinforce the model's utility in yield prediction, making it a valuable tool for precision agriculture. This nuanced approach highlights the superior predictive accuracy of PLSR, especially as the crop approaches maturation, and advocates for its deployment in the later growth stages of wheat to achieve optimal yield predictions.

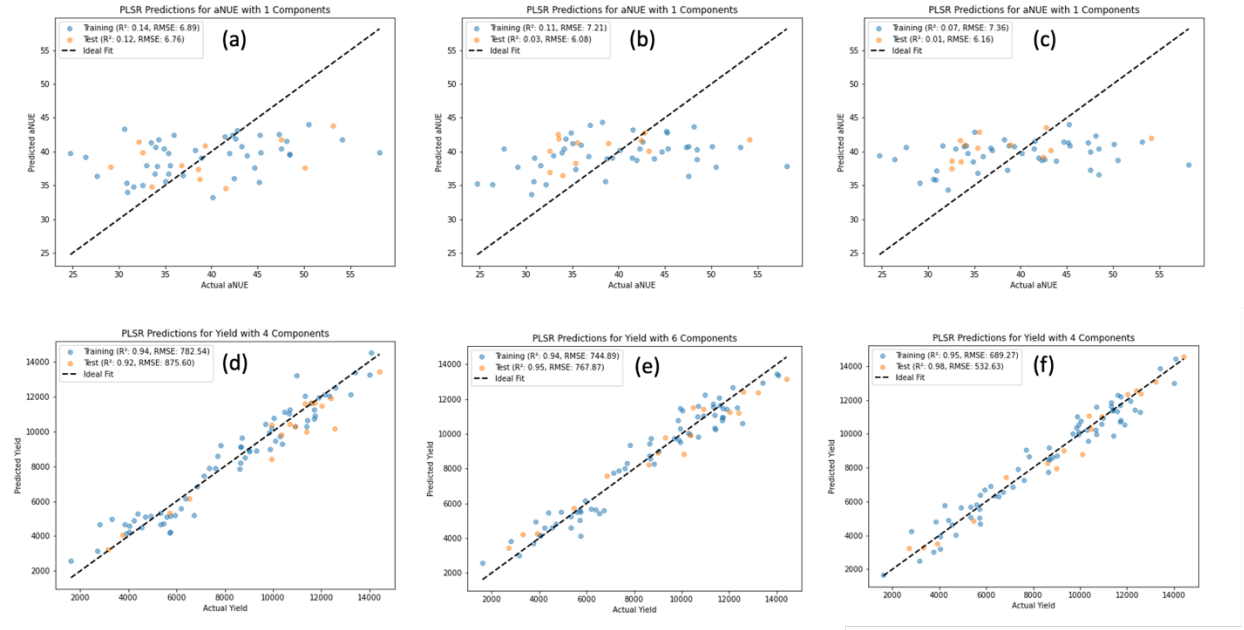

Fig 2. Comparison of the prediction of aNUE and GY using different PLSR models for the training and test datasets. (a) The prediction of aNUE using early PLSR model for the training dataset and test dataset; (b) The prediction of aNUE using medium PLSR model for the training dataset and test dataset; (c) The prediction of aNUE using early PLSR model for the training dataset and test dataset;; (d) The prediction of GY using early PLSR model for the training dataset and test dataset; (e) The prediction of GY using medium PLSR model for the training dataset and test dataset; (f) The prediction of GY using late PLSR model for the training dataset and test dataset.

3.2.2. Random Forest

The Random Forest models exhibit high predictive accuracy for both aNUE (Fig.3) and yield (Fig.4), with strong correlations between predicted and actual values across all growth stages. The R^2 values indicate that the models explain a significant proportion of the variance in the data. The relatively low RMSE values further suggest that the predictions are close to the actual values.

For aNUE (Fig.3), the models show the highest predictive accuracy in the medium stage, with R^2

= 0.73and RMSE = 3.57 for the test set. This is followed by the early stage, with R^2 = 0.61 and RMSE = 4.27 for the training set and R^2 = 0.56 and RMSE = 5.59 for the test set. The late stage shows R^2 = 0.57 and RMSE = 4.89 for the training set and R^2 = 0.63 and RMSE = 3.39 for the test set, indicating slightly lower but still substantial predictive power.

For yield (Fig.4), the models demonstrate exceptional predictive accuracy. The medium stage models achieve R^2 = 0.99 for both the training set and the test set, indicating perfect or near-perfect predictions. The late stage models achieve R^2 = 0.88for the training set and R^2 = 0.95 for the test set, showing very high accuracy. The early stage models also perform excellently, with R^2 = 0.75 for the training set and R^2 = 0.61 for the test set.

These results underscore the utility of Random Forest models in predicting key phenotyping traits. The models' ability to integrate complex spectral data and manage multicollinearity makes them robust frameworks for yield and efficiency predictions across different growth stages. The high correlation coefficients with actual values highlight the models' effectiveness, particularly in capturing the essential variations in the data that are critical for accurate predictions.

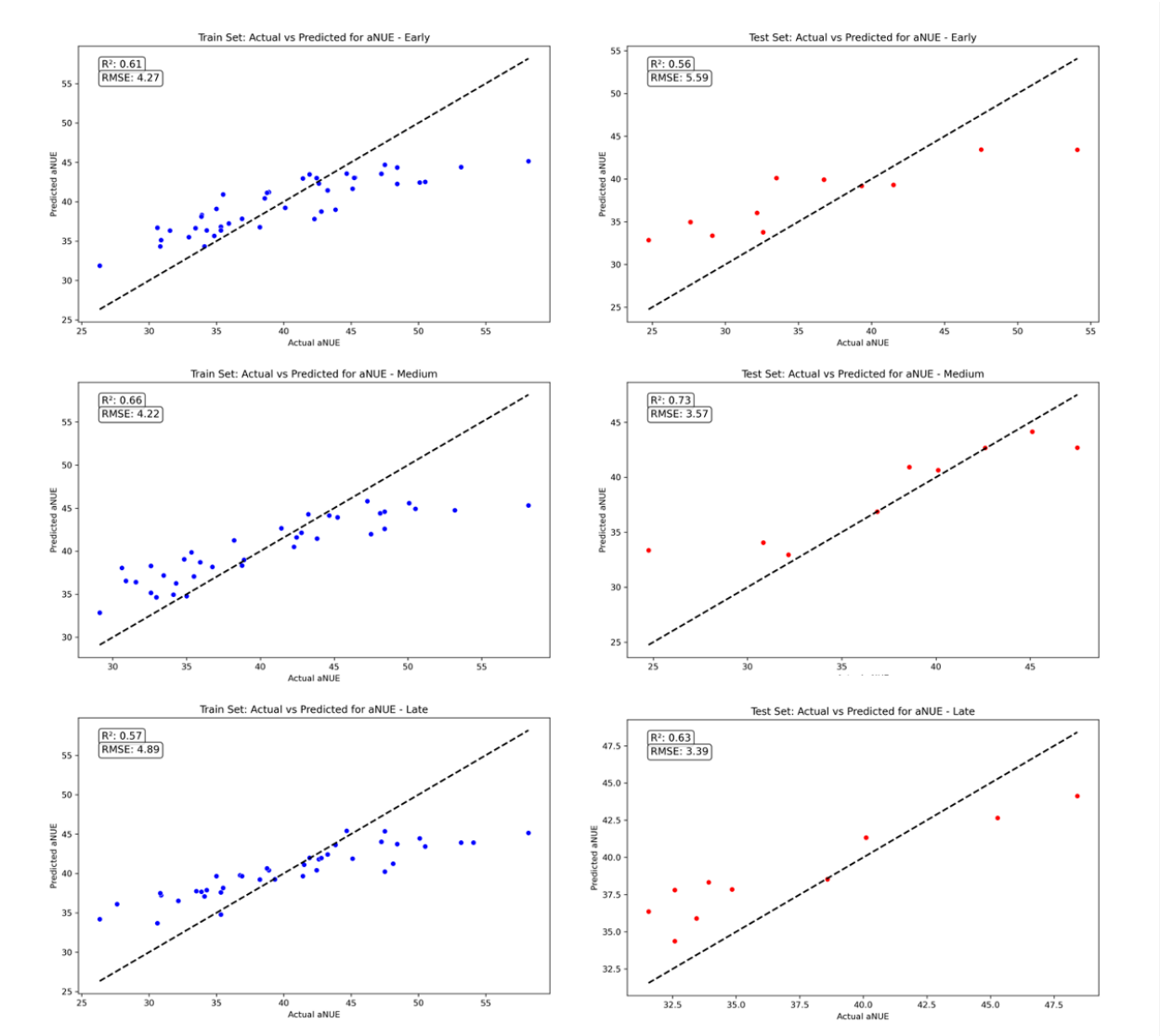

Fig 3. Comparison of the prediction of aNUE using different Random Forestry models for the training and test datasets.

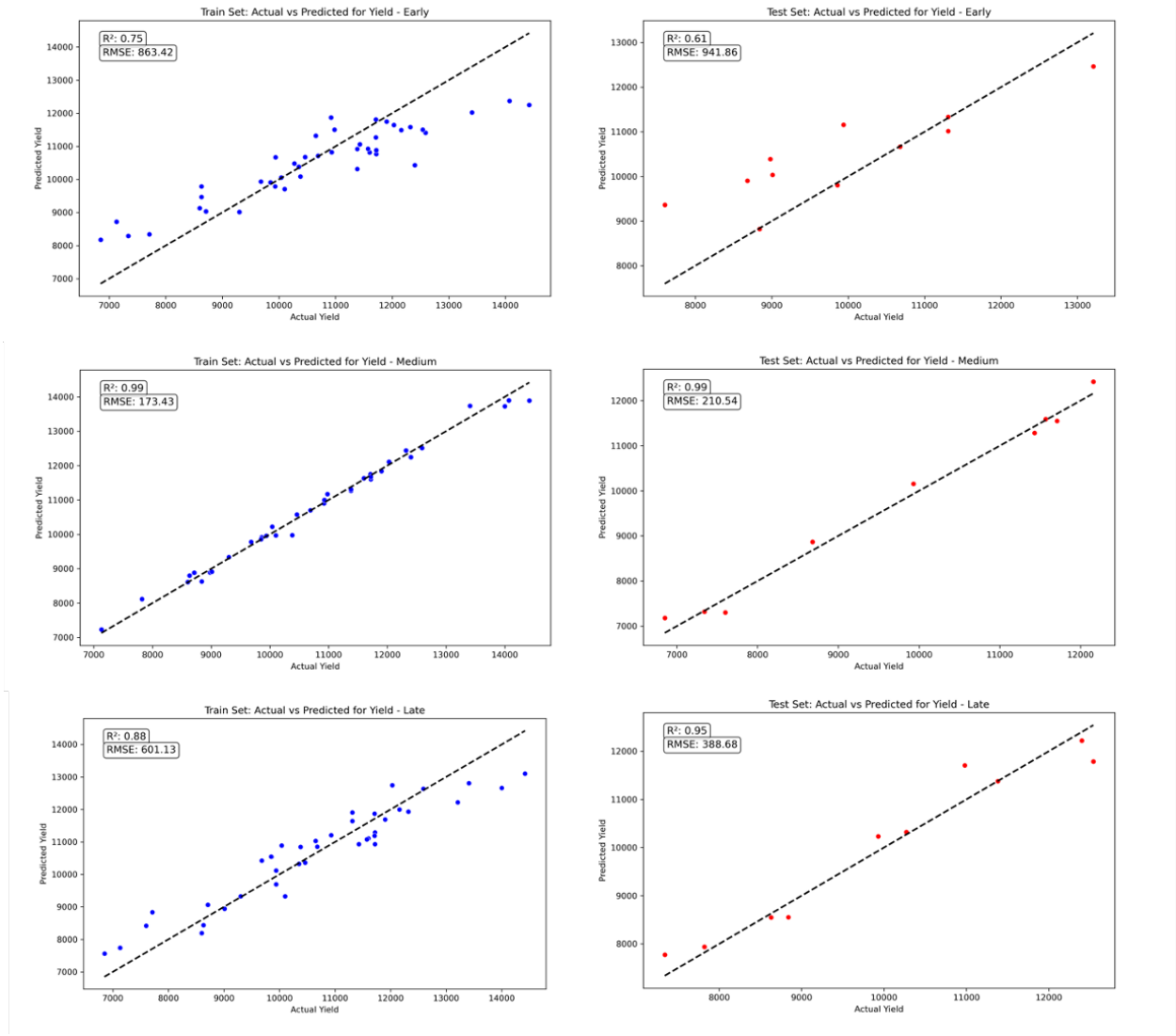

Fig 4. Comparison of the prediction of GY using different RF models for the training and test datasets.

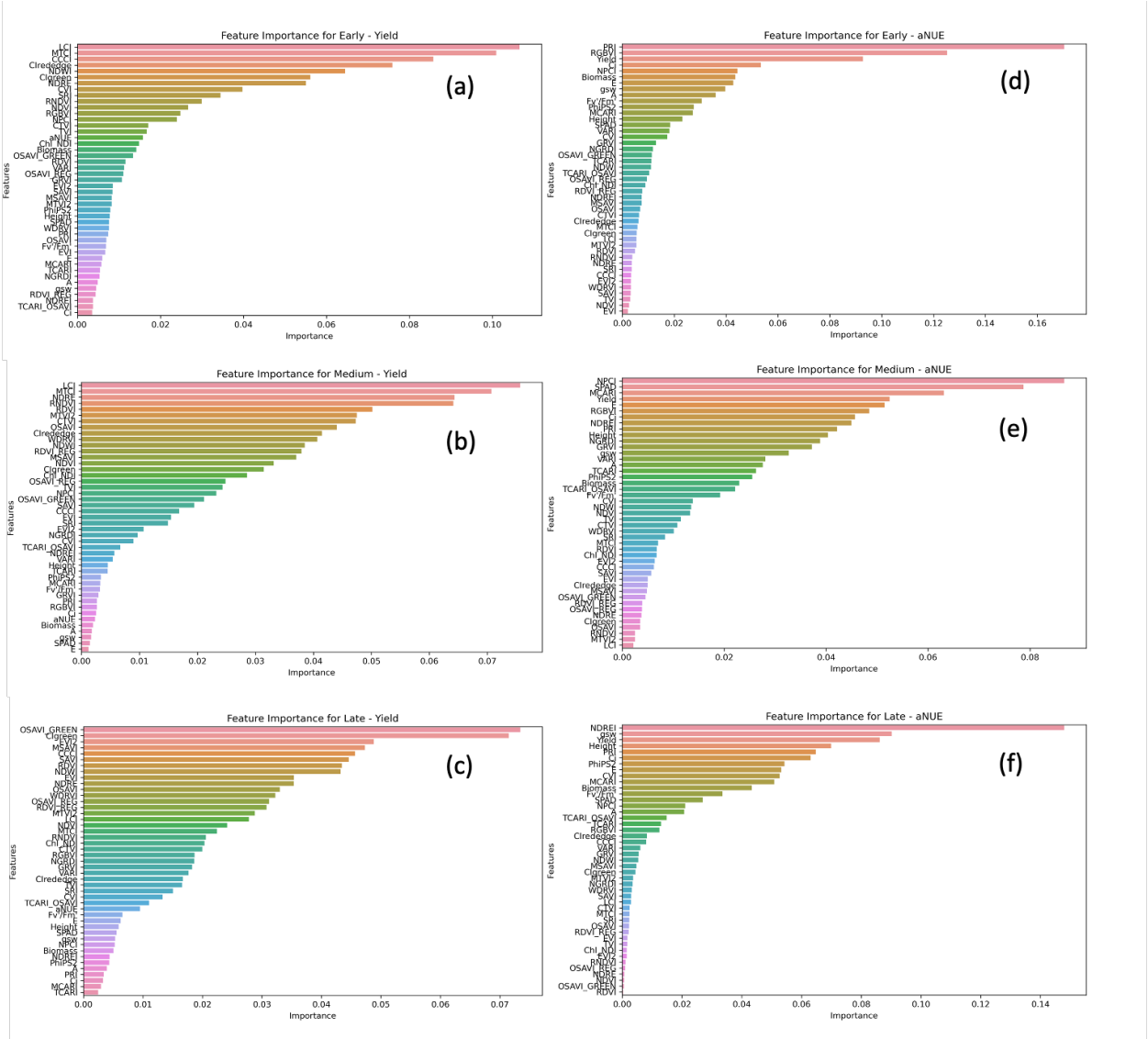

Fig 5. Comparison of the prediction of GY and aNUE using different RF models for the training and test datasets.

The provided images (Fig.5) depict the Variable Importance in Projection (VIP) scores, also known as feature importances, from the Random Forest models used to predict GY and aNUE at different growth stages. The feature importance scores help identify which variables contribute most to the model's predictions. The consistent importance of AGB, PhiPS2, Ci, and Fv'/Fm' across stages highlights these variables as key indicators of winter wheat phenotyping. The results underscore the utility of Random Forest models in identifying critical features for yield and aNUE predictions.

4.Conclusions

The study highlights the effectiveness of advanced statistical models in predicting key agronomic traits in winter wheat. The strong correlations identified between photosynthetic parameters, vegetation indices, and chlorophyll content emphasize the importance of these variables in phenotypes monitoring. The PLSR and RF models demonstrated substantial predictive power, particularly for grain yield, underscoring their utility in yield and aNUE estimation. The findings advocate for the deployment of these models in later growth stages to optimize yield predictions and enhance crop management practices. The consistent importance of AGB, PhiPS2, Ci, and Fv'/Fm' across different stages further validates these parameters as crucial indicators for winter wheat phenotyping.

References

1. The Basic Principles of Photosynthetic Energy Storage. In *Molecular Mechanisms of Photosynthesis*; 2002; pp. 1-10.
2. GU, J.; YIN, X.; STOMPH, T.-J.; STRUIK, P.C. Can exploiting natural genetic variation in leaf photosynthesis contribute to increasing rice productivity? A simulation analysis. *Plant, Cell & Environment* **2014**, *37*, 22-34, doi:https://doi.org/10.1111/pce.12173.
3. Lawson, T.; Kramer, D.M.; Raines, C.A. Improving yield by exploiting mechanisms underlying natural variation of photosynthesis. *Current Opinion in Biotechnology* **2012**, *23*, 215-220, doi:https://doi.org/10.1016/j.copbio.2011.12.012.
4. Flood, P.J.; Harbinson, J.; Aarts, M.G.M. Natural genetic variation in plant photosynthesis. *Trends in Plant Science* **2011**, *16*, 327-335, doi:https://doi.org/10.1016/j.tplants.2011.02.005.
5. Zhu, X.-G.; Long, S.P.; Ort, D.R. Improving Photosynthetic Efficiency for Greater Yield. *Annual Review of Plant Biology* **2010**, *61*, 235-261, doi:10.1146/annurev-arplant-042809-112206.
6. Furbank, R.T.; Sharwood, R.; Estavillo, G.M.; Silva-Perez, V.; Condon, A.G. Photons to food: genetic improvement of cereal crop photosynthesis. *Journal of Experimental Botany* **2020**, *71*, 2226-2238, doi:10.1093/jxb/eraa077.
7. Tarvainen, L.; Räntfors, M.; Wallin, G. Seasonal and within-canopy variation in shoot-scale resource-use efficiency trade-offs in a Norway spruce stand. *Plant, Cell & Environment* **2015**, *38*, 2487-2496, doi:https://doi.org/10.1111/pce.12565.
8. CARMO-SILVA, E.; SCALES, J.C.; MADGWICK, P.J.; PARRY, M.A.J. Optimizing Rubisco and its regulation for greater resource use efficiency. *Plant, Cell & Environment* **2015**, *38*, 1817-1832, doi:https://doi.org/10.1111/pce.12425.
9. Pennisi, G.; Blasioli, S.; Cellini, A.; Maia, L.; Crepaldi, A.; Braschi, I.; Spinelli, F.; Nicola, S.; Fernandez, J.A.; Stanghellini, C.; et al. Unraveling the Role of Red:Blue LED Lights on Resource Use Efficiency and Nutritional Properties of Indoor Grown Sweet Basil. *Frontiers in Plant Science* **2019**, *10*, doi:10.3389/fpls.2019.00305.
10. Donohue, R.J.; Roderick, M.L.; McVicar, T.R.; Yang, Y. A simple hypothesis of how leaf and canopy-level transpiration and assimilation respond to elevated CO2 reveals distinct response patterns between disturbed and undisturbed vegetation. *Journal of Geophysical Research: Biogeosciences* **2017**, *122*, 168-184, doi:https://doi.org/10.1002/2016JG003505.
11. Tausz-Posch, S.; Armstrong, R.; Tausz, M. Nutrient Use and Nutrient Use Efficiency of Crops in a High CO2 Atmosphere. In *Nutrient Use Efficiency in Plants: Concepts and Approaches*, Hawkesford, M.J., Kopriva, S., De Kok, L.J., Eds.; Springer International Publishing: Cham, 2014; pp. 229-252.
12. Tanaka, Y.; Sugano, S.S.; Shimada, T.; Hara-Nishimura, I. Enhancement of leaf photosynthetic capacity through increased stomatal density in Arabidopsis. *New Phytologist* **2013**, *198*, 757-764, doi:https://doi.org/10.1111/nph.12186.
13. Yamori, W.; Shikanai, T. Physiological Functions of Cyclic Electron Transport Around Photosystem I in Sustaining Photosynthesis and Plant Growth. *Annual Review of Plant Biology* **2016**, *67*, 81-106, doi:10.1146/annurev-arplant-043015-112002.
14. Guidi, L.; Lo Piccolo, E.; Landi, M. Chlorophyll Fluorescence, Photoinhibition and Abiotic Stress: Does it Make Any Difference the Fact to Be a C3 or C4 Species? *Frontiers in Plant Science* **2019**, *10*, doi:10.3389/fpls.2019.00174.
15. Bauriegel, E.; Giebel, A.; Herppich, W. Rapid Fusarium head blight detection on winter wheat ears using chlorophyll fl uorescence imaging. *Journal of Applied Botany and Food Quality* **2010**, *83*, 196-203.
16. Yao, J.; Sun, D.; Cen, H.; Xu, H.; Weng, H.; Yuan, F.; He, Y. Phenotyping of Arabidopsis Drought Stress Response Using Kinetic Chlorophyll Fluorescence and Multicolor Fluorescence Imaging. *Frontiers in Plant Science* **2018**, *9*, doi:10.3389/fpls.2018.00603.
17. Baker, N.R. Chlorophyll Fluorescence: A Probe of Photosynthesis In Vivo. *Annual Review of Plant Biology* **2008**, *59*, 89-113, doi:10.1146/annurev.arplant.59.032607.092759.
18. Sánchez-Moreiras, A.M.; Graña, E.; Reigosa, M.J.; Araniti, F. Imaging of Chlorophyll a Fluorescence in Natural Compound-Induced Stress Detection. *Frontiers in Plant Science* **2020**, *11*, doi:10.3389/fpls.2020.583590.
19. Guidi, L.; Calatayud, A. Non-invasive tools to estimate stress-induced changes in photosynthetic performance in plants inhabiting Mediterranean areas. *Environmental and Experimental Botany* **2014**, *103*, 42-52, doi:https://doi.org/10.1016/j.envexpbot.2013.12.007.
20. Yue, J.; Yang, G.; Tian, Q.; Feng, H.; Xu, K.; Zhou, C. Estimate of winter-wheat above-ground biomass based on UAV ultrahigh-ground-resolution image textures and vegetation indices. *ISPRS Journal of Photogrammetry and Remote Sensing* **2019**, *150*, 226-244, doi:https://doi.org/10.1016/j.isprsjprs.2019.02.022.
21. Walter, J.; Edwards, J.; McDonald, G.; Kuchel, H. Photogrammetry for the estimation of wheat biomass and harvest index. *Field Crops Research* **2018**, *216*, 165-174, doi:https://doi.org/10.1016/j.fcr.2017.11.024.
22. Tilly, N.; Aasen, H.; Bareth, G. Fusion of Plant Height and Vegetation Indices for the Estimation of Barley Biomass. *Remote Sensing* **2015**, *7*, 11449-11480.
23. Vatter, T.; Gracia-Romero, A.; Kefauver, S.C.; Nieto-Taladriz, M.T.; Aparicio, N.; Araus, J.L. Preharvest phenotypic prediction of grain quality and yield of durum wheat using multispectral imaging. *The Plant Journal* **2022**, *109*, 1507-1518, doi:https://doi.org/10.1111/tpj.15648.

24. Zhang, J.; Hu, Y.; Li, F.; Fue, K.G.; Yu, K. Meta-Analysis Assessing Potential of Drone Remote Sensing in Estimating Plant Traits Related to Nitrogen Use Efficiency. *Remote Sensing* **2024**, *16*, 838.
25. Bendig, J.; Bolten, A.; Bennertz, S.; Broscheit, J.; Eichfuss, S.; Bareth, G. Estimating Biomass of Barley Using Crop Surface Models (CSMs) Derived from UAV-Based RGB Imaging. *Remote Sensing* **2014**, *6*, 10395-10412.
26. Araus, J.L.; Cairns, J.E. Field high-throughput phenotyping: the new crop breeding frontier. *Trends in Plant Science* **2014**, *19*, 52-61, doi:https://doi.org/10.1016/j.tplants.2013.09.008.
27. Houle, D.; Govindaraju, D.R.; Omholt, S. Phenomics: the next challenge. *Nature Reviews Genetics* **2010**, *11*, 855-866, doi:10.1038/nrg2897.
28. Salter, W.T.; Gilbert, M.E.; Buckley, T.N. A multiplexed gas exchange system for increased throughput of photosynthetic capacity measurements. *Plant Methods* **2018**, *14*, 80, doi:10.1186/s13007-018-0347-y.
29. Paudel, D.; Boogaard, H.; de Wit, A.; van der Velde, M.; Claverie, M.; Nisini, L.; Janssen, S.; Osinga, S.; Athanasiadis, I.N. Machine learning for regional crop yield forecasting in Europe. *Field Crops Research* **2022**, *276*, 108377, doi:https://doi.org/10.1016/j.fcr.2021.108377.
30. Herzig, P.; Borrmann, P.; Knauer, U.; Klück, H.-C.; Kilias, D.; Seiffert, U.; Pillen, K.; Maurer, A. Evaluation of RGB and Multispectral Unmanned Aerial Vehicle (UAV) Imagery for High-Throughput Phenotyping and Yield Prediction in Barley Breeding. *Remote Sensing* **2021**, *13*, 2670.
31. Prey, L.; Schmidhalter, U. Simulation of satellite reflectance data using high-frequency ground based hyperspectral canopy measurements for in-season estimation of grain yield and grain nitrogen status in winter wheat. *ISPRS Journal of Photogrammetry and Remote Sensing* **2019**, *149*, 176-187, doi:https://doi.org/10.1016/j.isprsjprs.2019.01.023.
32. Makanza, R.; Zaman-Allah, M.; Cairns, J.E.; Magorokosho, C.; Tarekegne, A.; Olsen, M.; Prasanna, B.M. High-Throughput Phenotyping of Canopy Cover and Senescence in Maize Field Trials Using Aerial Digital Canopy Imaging. *Remote Sensing* **2018**, *10*, 330.
33. Liu, S.; Baret, F.; Allard, D.; Jin, X.; Andrieu, B.; Burger, P.; Hemmerlé, M.; Comar, A. A method to estimate plant density and plant spacing heterogeneity: application to wheat crops. *Plant Methods* **2017**, *13*, 38, doi:10.1186/s13007-017-0187-1.
34. Liu, W.; Li, Y.; Liu, J.; Jiang, J. Estimation of Plant Height and Aboveground Biomass of Toona sinensis under Drought Stress Using RGB-D Imaging. *Forests* **2021**, *12*, 1747.